NASA/TM—2017-219514

Residual Stresses in a NiCrY-Coated Powder Metallurgy Disk Superalloy

Timothy P. Gabb, Richard B. Rogers, James A. Nesbitt, and Bernadette J. Puleo
Glenn Research Center, Cleveland, Ohio

Robert A. Miller
Vantage Partners, LLC, Brook Park, Ohio

Jack Telesman and Susan L. Draper
Glenn Research Center, Cleveland, Ohio

Ivan E. Locci
University of Toledo, Toledo, Ohio

June 2017

NASA STI Program . . . in Profile

Since its founding, NASA has been dedicated to the advancement of aeronautics and space science. The NASA Scientific and Technical Information (STI) Program plays a key part in helping NASA maintain this important role.

The NASA STI Program operates under the auspices of the Agency Chief Information Officer. It collects, organizes, provides for archiving, and disseminates NASA's STI. The NASA STI Program provides access to the NASA Technical Report Server—Registered (NTRS Reg) and NASA Technical Report Server—Public (NTRS) thus providing one of the largest collections of aeronautical and space science STI in the world. Results are published in both non-NASA channels and by NASA in the NASA STI Report Series, which includes the following report types:

- TECHNICAL PUBLICATION. Reports of completed research or a major significant phase of research that present the results of NASA programs and include extensive data or theoretical analysis. Includes compilations of significant scientific and technical data and information deemed to be of continuing reference value. NASA counter-part of peer-reviewed formal professional papers, but has less stringent limitations on manuscript length and extent of graphic presentations.

- TECHNICAL MEMORANDUM. Scientific and technical findings that are preliminary or of specialized interest, e.g., "quick-release" reports, working papers, and bibliographies that contain minimal annotation. Does not contain extensive analysis.

- CONTRACTOR REPORT. Scientific and technical findings by NASA-sponsored contractors and grantees.

- CONFERENCE PUBLICATION. Collected papers from scientific and technical conferences, symposia, seminars, or other meetings sponsored or co-sponsored by NASA.

- SPECIAL PUBLICATION. Scientific, technical, or historical information from NASA programs, projects, and missions, often concerned with subjects having substantial public interest.

- TECHNICAL TRANSLATION. English-language translations of foreign scientific and technical material pertinent to NASA's mission.

For more information about the NASA STI program, see the following:

- Access the NASA STI program home page at http://www.sti.nasa.gov

- E-mail your question to help@sti.nasa.gov

- Fax your question to the NASA STI Information Desk at 757-864-6500

- Telephone the NASA STI Information Desk at 757-864-9658

- Write to:
  NASA STI Program
  Mail Stop 148
  NASA Langley Research Center
  Hampton, VA 23681-2199

Residual Stresses in a NiCrY-Coated Powder Metallurgy Disk Superalloy

Timothy P. Gabb, Richard B. Rogers, James A. Nesbitt, and Bernadette J. Puleo
Glenn Research Center, Cleveland, Ohio

Robert A. Miller
Vantage Partners, LLC, Brook Park, Ohio

Jack Telesman and Susan L. Draper
Glenn Research Center, Cleveland, Ohio

Ivan E. Locci
University of Toledo, Toledo, Ohio

National Aeronautics and
Space Administration

Glenn Research Center
Cleveland, Ohio 44135

June 2017

Acknowledgments

Level of Review: This material has been technically reviewed by technical management.

Available from

NASA STI Program	National Technical Information Service
Mail Stop 148	5285 Port Royal Road
NASA Langley Research Center	Springfield, VA 22161
Hampton, VA 23681-2199	703-605-6000

This report is available in electronic form at http://www.sti.nasa.gov/ and http://ntrs.nasa.gov/

Residual Stresses in a NiCrY-Coated Powder Metallurgy Disk Superalloy

Timothy P. Gabb, Richard B. Rogers, James A. Nesbitt, and Bernadette J. Puleo
National Aeronautics and Space Administration
Glenn Research Center
Cleveland, Ohio 44135

Robert A. Miller
Vantage Partners, LLC
Brook Park, Ohio 44142

Jack Telesman and Susan L. Draper
National Aeronautics and Space Administration
Glenn Research Center
Cleveland, Ohio 44135

Ivan E. Locci
University of Toledo
Toledo, Ohio 43606

Abstract

Protective ductile coatings will be necessary to mitigate oxidation and corrosion attack on superalloy disks exposed to increasing operating temperatures in some turbine engine environments. However, such coatings must be resistant to harmful surface cracking during service. The objective of this study was to investigate how residual stresses evolve in such coatings. Cylindrical gage fatigue specimens of powder metallurgy-processed disk superalloy LSHR were coated with a NiCrY coating, shot peened, and then subjected to fatigue in air at room and high temperatures. The effects of shot peening and fatigue cycling on average residual stresses and other aspects of the coating were assessed. Shot peening did induce beneficial compressive residual stresses in the coating and substrate. However, these stresses became more tensile in the coating with subsequent heating, contributing to cracking of the coating in long intervals of cycling at 760 °C. Yet, substantial compressive residual stresses remained in the substrate adjacent to the coating, sufficient to suppress fatigue cracking there. The coating continued to protect the substrate from hot corrosion pitting, even after fatigue cracks initiated in the coating.

Introduction

The design of powder metallurgy (PM) disk superalloys to allow increased engine operating temperatures requires improvements of their strength, creep, and fatigue resistance (Ref. 1). However, disk application temperatures of 700 °C and higher can enhance oxidation and also activate hot corrosion attack modes in harmful environments, to also become important design limitations.

Several studies have shown that oxidation from exposures at 700 °C and higher can impair the fatigue resistance of disk superalloys (Refs. 2 and 3). This oxidation encompassed the formation of oxide layers and changes in superalloy chemistry and phases adjacent to the oxide layers. While the formation of chromium oxide is known to be protective, other nickel, cobalt, and titanium oxides can also form that are considered not protective. In addition, selective oxidation of certain elements can result in the formation of a zone adjoining the oxide layers of weakened gamma phase without gamma prime precipitates, which can be recrystallized to a finer grain size than the original disk alloy grains. The grain boundaries in this zone can be susceptible to cracking during fatigue at high temperatures, related to these changes and a lack of $M_{23}C_6$ carbides (Ref. 4). So collectively, these features can lower the mechanical fatigue resistance at the surface of disk superalloys.

Type II hot corrosion attack can occur at 700 °C to nearly 800 °C on superalloy surfaces (Refs. 5 and 6) by the melting of ingested deposits containing mixtures of sodium-, magnesium-, and calcium-sulfates, as well as by direct impingement of SO_2-containing exhaust gas. However, SO_2 gas is not necessary for hot corrosion attack by these deposits. Here, the liquid sulfates can react with surface oxides to make the oxide go into solution and thereby be rendered non-protective. This allows penetration of the newly exposed superalloy surface. The attack can be further enhanced at the grain boundaries in superalloys in certain conditions. Pits can form in some conditions, while general corrosion can otherwise occur (Ref. 7). The pits can act as geometric stress concentration sites, which encourage cracks to initiate during mechanical fatigue loading. Pitting and uniform corrosion can significantly reduce the fatigue resistance of disk superalloys (Refs. 3, 8 to 11).

For susceptible locations, a suitable metallic coating could provide protection of exposed disk surfaces from this oxidation and corrosion for relevant temperatures and environments. PtAl, NiAl, and NiCoCrAlY (Ref. 12) coatings have been extensively developed to protect superalloy airfoils from oxidation and corrosion. These coatings have also been used to serve as "bond coatings" between the superalloy and thermal barrier coatings. However, these coatings have lower ductility and fatigue resistance than turbine disk superalloys, for likely turbine disk temperatures extending up to 760 °C. It is essential that any candidate for protective coating not impair the mechanical properties and functions of the rotating disk, which is subjected to high thermal strains and cyclic stresses in each flight or service cycle. More specifically, this coating must not harm the fatigue resistance of the disk surfaces upon which it is applied, as disks are fatigue-limited and fracture critical in aero-propulsion applications.

Disk surfaces can be machined using various processes including point turning, drilling, broaching, and low stress grinding (Ref. 13). Many of these machined surfaces are subsequently shot peened. Shot peening can produce a consistent surface finish and impart beneficial compressive residual stresses near the treated surfaces, that can impede fatigue cracking there (Refs. 14 and 15). The application of a coating to protect selected disk surfaces would need to be included within this fabrication process path. One possible approach would be to apply the coating after machining of a disk surface location, before shot peening. After coating, the disk including its coated surfaces could then be shot peened. The residual stresses and roughness generated by shot peening within the coating would need to be evaluated for such an approach, in order to minimize the coating's effect on the disk's resistance to fatigue cracking, while still offering protection from oxidation and corrosion attack. The evolution of the coating's residual stresses and surface roughness with heating and fatigue cycling would need to be considered in this.

The objective of the study was to determine the residual stresses, fatigue resistance, and corrosion resistance of a powder metal nickel-based superalloy coated with a NiCrY coating and then shot peened. The effects of specimen processing, heating, and fatigue cycling on residual stresses, roughness, fatigue cracking, and hot corrosion resistance were evaluated.

Materials and Procedure

A nickel-chromium-yttrium coating was deposited on PM disk superalloy LSHR for this study. The LSHR test material had the compositions listed in Table 1. LSHR superalloy powder was atomized in argon by Special Metals, PCC, screened to –270 mesh, sealed in a stainless steel container, consolidated by hot isostatic pressing, extruded, and then segments were isothermally forged into flat disks (Ref. 16). Rectangular blanks about 13 mm square and 66 mm to 83 mm long were extracted from the as-forged disks. These blanks were supersolvus solution heat treated at 1171 °C for 2 h in a resistance heating furnace, then cooled in static air at an average cooling rate of 72 °C per min. They were subsequently aging heat treated at 855 °C for 4 h, followed by 775 °C for 8 h. The resulting LSHR grain microstructure

TABLE 1.—POWDER METAL SUPERALLOY LSHR COMPOSITION IN WEIGHT PERCENT

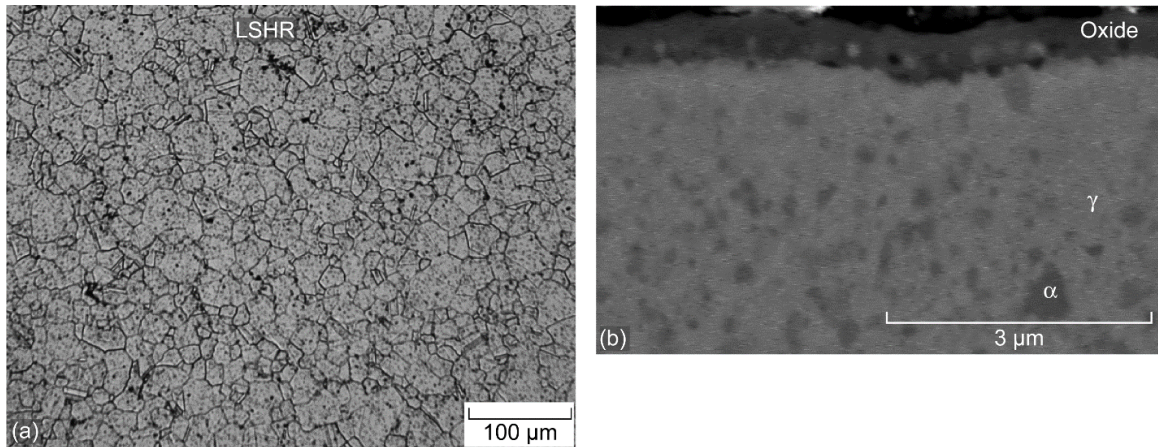| Alloy - wt.%	Al	B	C	Co	Cr	Fe	Mn	Mo	Ni	Nb	O	Si	S	Ta	Ti	V	W	Y	Zr
LSHR	3.54	0.027	0.045	20.40	12.30	0.07	0.00	2.71	Bal.	1.49	0.02	0.012	<.0010	1.52	3.45	0.0055	4.28	<.0005	0.05

Figure 1.—Test material microstructures: (a) LSHR superalloy after solution and aging heat treatments, with an average grain size of 15 μm, (b) typical microstructure showing γ and α phases of NiCrY coating, after shot peening and inter-diffusion heat treatment at 760 °C for 8 h.

is shown in Figure 1(a), for a metallographically prepared section swab-etched in Waterless Kalling's reagent. The heat treated material had an average linear intercept grain size of about 15 μm. Fatigue specimens having uniform gage sections 6.4 mm in diameter were then machined. The test specimens were all machined by low stress grinding, followed by longitudinal polishing with abrasive paper to a root mean square roughness of less than 0.2 μm.

High Power Impulse Magnetron Sputtering (HiPIMS) was employed by Southwest Research Institute to apply a Ni-45Cr-0.15Y (weight percent, nominal) coating. Prior to coating, the test specimen surface was prepared by grit blast using alumina grit. Both ends of each specimen were masked with metal foil so that only the reduced gauge test section was exposed for coating. A hang wire was attached to the metal masking foil. In the coater, the hang wire for each specimen was attached to a planetary rotating fixture to produce uniform coating thicknesses on the individual samples. Five bars were coated during a single coating run. Two coating runs were made under identical run conditions.

Coated and comparative uncoated fatigue test specimens were consistently shot peened at Metal Improvement Company according to AMS 2432 using conditioned cut stainless steel wire (CCW14) at an intensity of 16 N and coverage of 200 percent. Here, 100 percent coverage indicates 100 percent of the surface area has been impacted, while 200 percent indicates 200 percent of the time of shot peening needed to attain this 100 percent of coverage was expended (Ref. 17). After shot peening, all test specimens were heat treated at 760 °C for 8 h in a low partial pressure of oxygen, to promote inter-diffusion between the coating and substrate for the coated specimens, and also to form a protective chromium-oxide layer on the surface.

The microstructure of the coating after these preparation steps is compared to that of the LSHR in Figure 1(b). The coating had a mean thickness of 26.5 μm with a 95 percent confidence interval of ±1.3 μm, using measurements of sections from unexposed test specimens. It consisted of a γ nickel-rich matrix with about 15 area percent of α chromium-rich precipitates. These α precipitates had a wide range of sizes, with equivalent radius extending from 0.01 to 0.31 μm.

Fatigue cycling was conducted in air on all test specimens, using a servo-hydraulic test machine with a resistance heating furnace integrated to enclose the specimen and specimen grips. Stress was consistently cycled between maximum and minimum stress values of 841 and –427 MPa in each cycle using a saw-tooth waveform at a frequency of 0.33 Hz. These stresses corresponded to the stabilized maximum and minimum stresses produced by tests run on this material with strain cycled at a strain range of 0.76 percent and strain ratio (minimum/maximum strain) of 0 at 760 °C. However, in the present tests stress was cycled, and an extensometer was not used to contact the coated specimen surface for measuring strain, to avoid impingement of the coating. In prior tests at these conditions, specimens of this material which had been prepared, coated, shot peened and heat treated as described here had a mean fatigue life of about 70,000 cycles at 760 °C. Uncoated specimens that were only machined, shot peened, and

subjected to the same heat treatment as used for coated specimens also had a mean fatigue life of about 70,000 cycles. So in the present tests, separate specimens were stopped at 14, 700, and 35,000 cycles. These cycle intervals represent 0.02, 1, and 50 percent of the average fatigue life of 70,000 cycles that had been measured at 760 °C. Different specimens were interrupted at these different intervals of fatigue cycles, which were performed at 760 °C and also at room temperature.

Selected coated and uncoated fatigue test specimens were examined as-coated, after shot peening, and after heat treatment at 760 °C for 8 h in a low partial pressure of oxygen, the starting condition before fatigue cycling. They were then later examined after the fatigue cycles. Residual stresses were measured at the gage surface using a Bruker D8 Discover (area detector) X-ray diffractometer aligned in accordance with the approach and error bounds specified in ASTM E 915-10, but applied to the side-inclination rather than iso-inclination method. Data was gathered using Mn Kα radiation and the (311) crystallographic plane on a specimen target area of 1.2 mm^2. Each residual stress dataset consisted of 24 area detector frames taken at 4 sample tilt (psi) angles (0°, 15°, 30°, and 45°) and 6 sample rotation (phi) angles (0°, 45°, 90°, 180°, 225°, and 270°). Sample X-ray penetration depths decreased with increasing psi angle, going from 19 to 13 μm in LSHR and from 30 to 21 μm in the coating, representing depths that correspond to a 99 percent contribution to the diffracted beam. These X-ray results were analyzed using the Bruker LEPTOS v.7 software. Peak width was measured using the TOPAS program. Average roughness was measured using a Zygo NewView 7200 white light interferometer, with a 10x objective lens magnification having a resolution of 0.001 μm. Gage surfaces were also examined using a JEOL 6100 scanning electron microscope (SEM) at magnifications up to 1000x.

After completion of these initial measurements, spots near one end of the gage surface were electro-polished to various depths, in order to measure the variation in residual stresses with depth from the surface. Electro-polishing was performed using a Proto Model 8818 Electrolytic Polisher, using a probe tip orifice of less than 4 mm in diameter. Assuming axial symmetry, the electro-polishing to various depths allowed comparisons of residual stress and peak width versus depth for different cases. The depth of each electro-polished spot was measured using the Zygo NewView 7200. The effect of removing material on the subsequently measured stresses was determined using appropriate stress relationships (Ref. 18), so that stresses could be corrected to account for this layer removal. Transverse sections were then sliced from the gage of each fatigue specimen, and metallographically prepared for examination in the SEM. Precipitate size and area fraction, as well as coating thicknesses, were measured using SigmaScan Pro image analysis software.

The remaining length of the gage section on each specimen was then subjected to an accelerated hot corrosion test. These specimen sections were corroded in air, by first coating them with a salt mixture of 59 wt% Na_2SO_4 and 41 wt% $MgSO_4$ applied at 2 mg/cm^2. They were then suspended horizontally in a resistance-heating tube furnace at 760 °C for 50 h. This salt lies at a eutectic composition with a melting point of 662 °C and was observed to melt and flow in previous testing at 760 °C. Previous work demonstrated that uncoated LSHR test specimen sections treated in this manner and tested at 760 °C in air nucleated and grew corrosion pits within just 24 h, which had a substantial effect on fatigue lives (Ref. 19). Coated and uncoated fatigue specimen sections which were given this corrosion for 50 h were again examined in the SEM for the presence of pits.

Results and Discussion

The effects of specimen preparation steps on surface conditions were first assessed. Typical SEM images of the surfaces are compared in Figure 2 after (a) initial machining, (b) machined plus shot peened plus heat treated, (c) initial coating, and (d) coated plus shot peened plus heat treated. Machining of the fatigue test specimens by low stress grinding and polishing in the axial direction produced very fine polishing grooves in the axial direction. Grit blasting and coating this surface eliminated the axial grooved texture producing a non-directional coating texture. Spits, or coating nodules (Fig. 2), were observed to be scattered on the surfaces for all coated test specimens. These are believed to form from random arcing
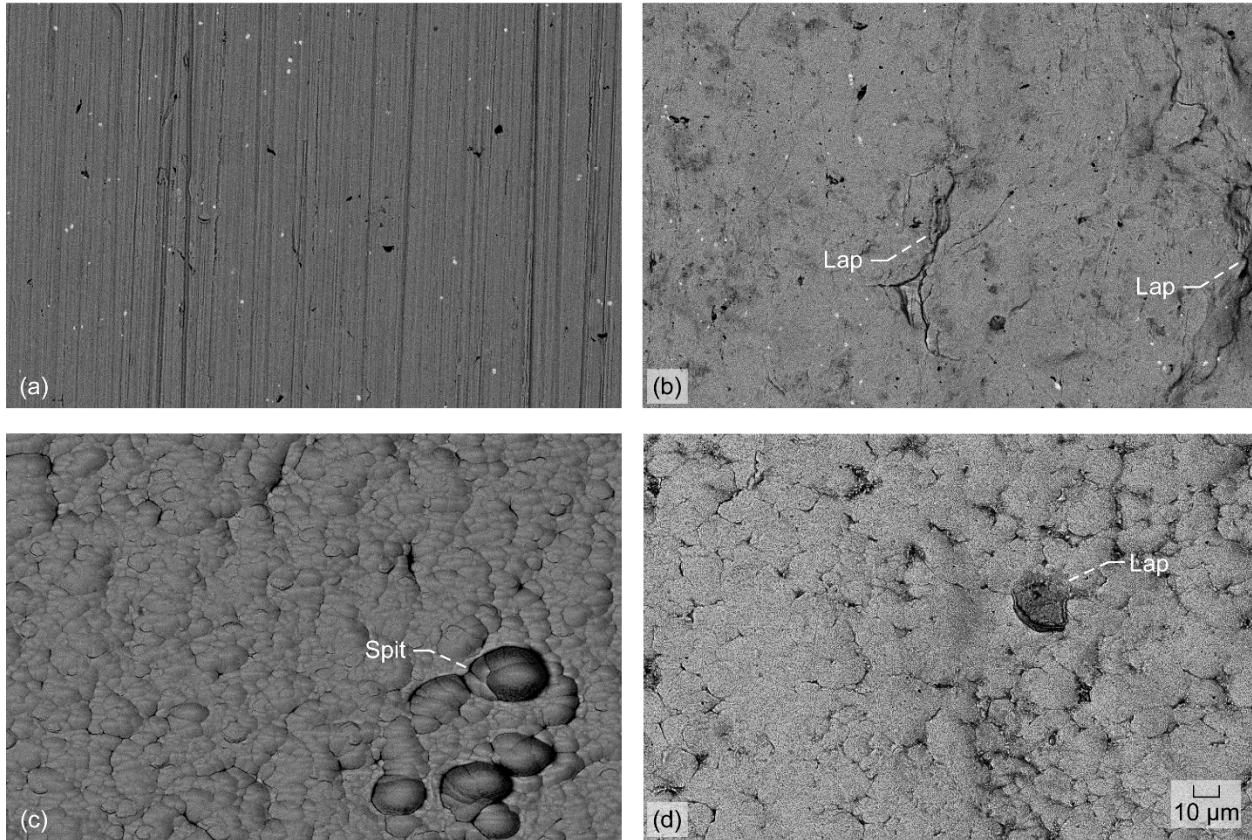
Figure 2.—Effects of specimen preparation steps on surface appearance. (a) uncoated specimen after machining, (b) uncoated specimen after machining, shot peening, and inter-diffusion heat treatment, (c) coated specimen after coating application, with "spits" from the coating process, (d) coated specimen after subsequent shot peening and inter-diffusion heat treatment. "Laps" from the shot peening process are indicated. Shot peening appeared to improve the uniformity of both surfaces. The fatigue loading direction is oriented vertically.

events in the plasma. Hence, deposition of the coating increased the roughness over that of the machined surface. The shot peened and heat treated surfaces were more uniform, with the formerly grooved and nodular surface textures mostly eliminated, being replaced with an undulating, dimpled texture. Shot peening of the coated surface resulted in folds of metal ("laps") sometimes occurring at the edges of dimples created by the impact of shot (Fig. 2). This shot peened texture was finer in scale for coated specimens than for uncoated specimens, apparently related to the prior fine scale nodular coated surface.

Associated average surface roughness and peak-to-valley roughness are compared in Figure 3. Although more uniform in texture, shot peening increased the corresponding roughness of uncoated specimens, and both roughness parameters became more similar for shot peened and heat-treated test specimens that were uncoated and coated, Figure 3.

The residual stresses measured at the surface also varied as a function of processing steps, as compared in Figure 4. Machining of the fatigue test specimens produced approximately –1100 MPa compressive residual stresses at the surface in both the axial and transverse directions. These compressive stresses remained after grit blasting. However, coating of this surface drastically changed the residual stresses, producing modest tensile surface residual stresses in the coating for both axial and transverse directions. It is recognized that various coating processes can themselves introduce varied residual stresses in coatings of similar composition. For example, compressive residual stresses near –500 MPa were reported in Ni-20Cr and Ni-50Cr coatings applied by cold spraying onto steel (Ref. 20). However, the present coating process utilized physical vapor deposition, which did not have the high speed impacts of solid powder particles such as in cold spraying. Subsequent shot peening produced comparable

compressive residual stresses for both uncoated and coated surfaces. Yet, final heat treatment at 760 °C for 8 h relaxed compressive surface residual stresses for both uncoated and coated surfaces. Ultimately, the fully prepared uncoated specimens had only modest compressive residual stresses measured at the surface of approximately –200 MPa. Fully prepared coated specimens had modest tensile residual stresses of about +200 MPa. The generation of compressive residual stresses in the coating by shot peening has been described for MCrAlY coatings applied by various processes (Ref. 21) and for NiCr coatings on superalloys (Ref. 22). However, the complete relaxation in the coating of these compressive stresses during subsequent exposures to the high temperature used in the present study was not reported or expected. The reasons for this response of the coating are being further investigated.
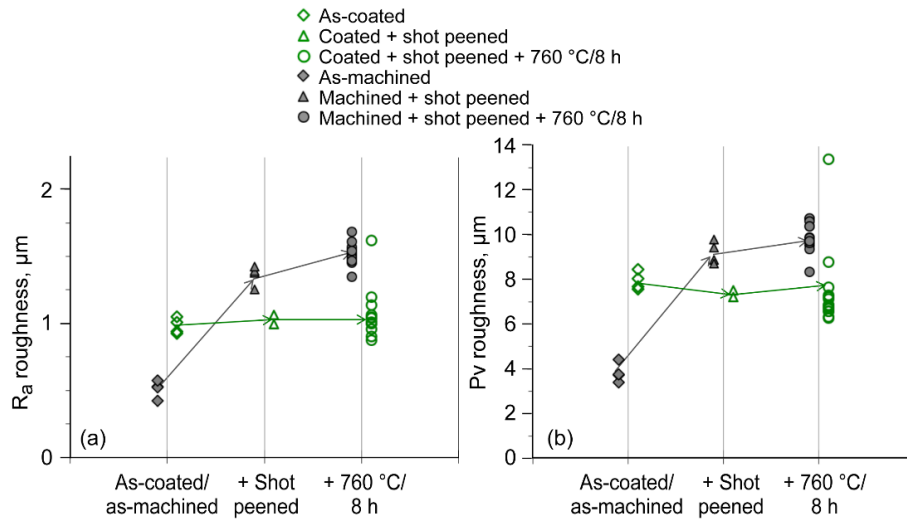

Figure 3.—Effects of specimen preparation steps on surface roughness (a) average roughness (R_a) and (b) Peak-to-valley roughness (Pv). Shot peening increased the roughness values of uncoated specimens (filled symbols), while roughness was maintained in coated specimens (hollow symbols).
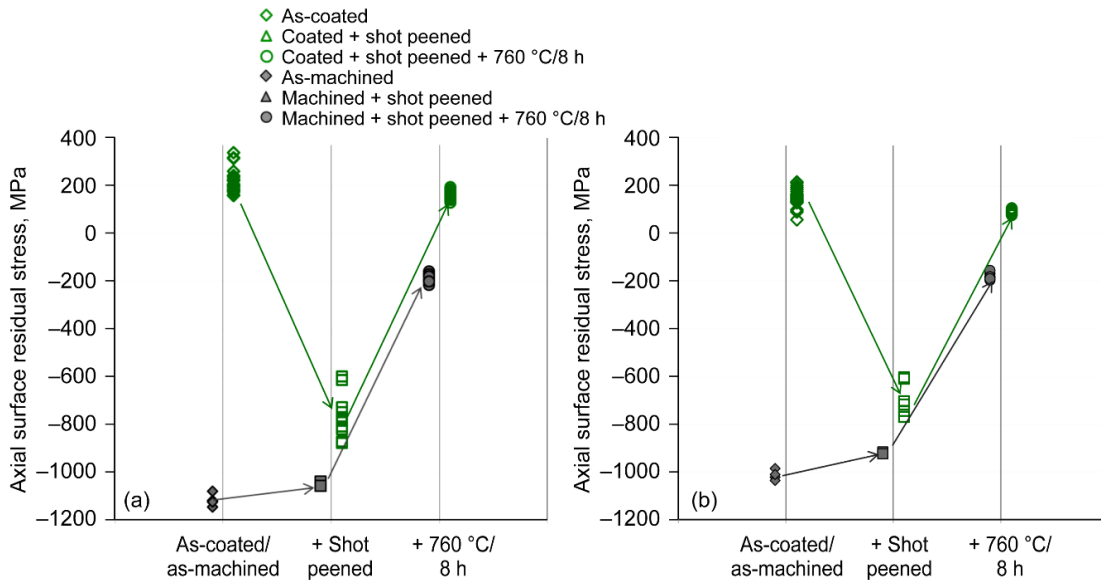

Figure 4.—Effects of specimen preparation steps on surface residual stresses in the (a) axial loading and (b) transverse directions. Shot peening produced closer compressive residual stresses for uncoated (filled symbols) and coated (hollow symbols) surfaces. Heat treatment at 760 °C for 8 h relaxed out much of these compressive residual stresses at the surface.
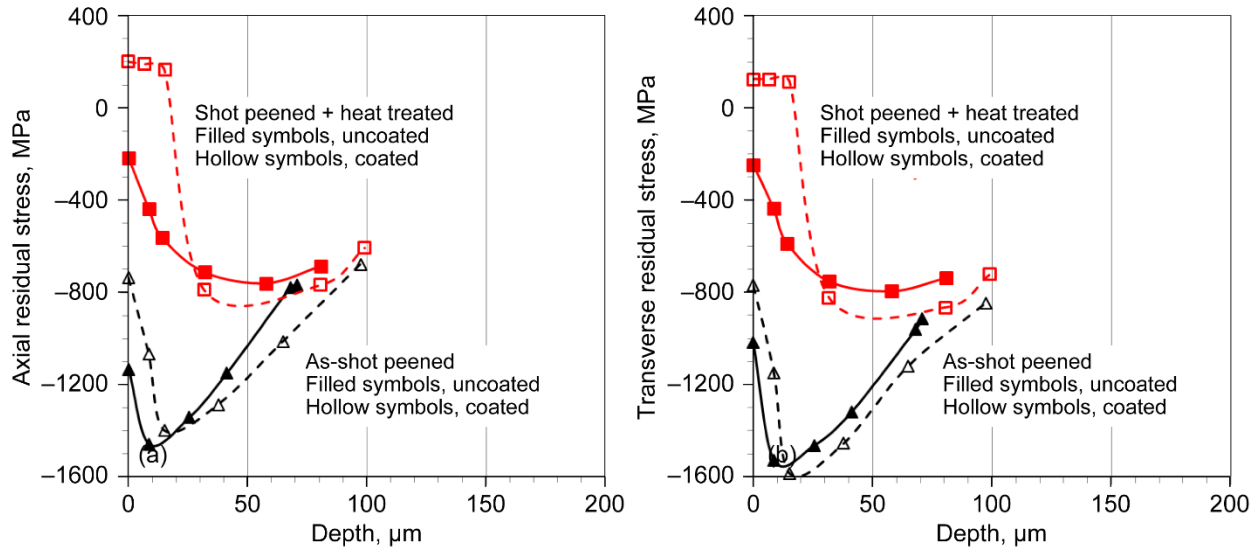
Figure 5.—Comparison of residual stresses near the surface for uncoated (filled symbols) and coated (hollow symbols) test specimens that have been shot peened, before (black symbols) and after (red symbols) the inter-diffusion heat treatment. Shot peening produced greater compressive (a) axial and (b) transverse residual stresses for uncoated and coated test specimens within the near-surface region of 100 μm. Substantial compressive residual stresses remained in the substrate after heat treatment, but the entire coating came into tension.

These surface measurements suggested less benefit of compressive residual stresses from shot peening remained after heat treating uncoated test specimens, and no benefit remained for coated test specimens, if these measurements were representative of the residual stress surface depth profiles. To determine the residual stress profiles, X-ray measurements were therefore repeated after electro-polishing to different depths of up to 100 μm from the surface. For both coated (filled symbols) and uncoated (hollow symbols) test specimens, axial and transverse residual stresses varied significantly with depth, when comparing shot peened test specimens before and after heat treatment, Figure 5. Shot peening (black symbols) produced beneficial compressive residual stresses for both uncoated and coated test specimens within the near-surface region of 100 μm depth, which were greater than those measured at the surface. The magnitudes of compressive axial and transverse stresses at and adjacent to the surface were reduced by the subsequent heat treatment (red symbols), especially within 25 μm of the surface for the coated specimens. At depths of over 25 μm, these reductions were more modest, and comparable for coated and uncoated specimens. Overall, substantial compressive residual stresses of at least –500 MPa remained for both coated and uncoated specimens at depths of about 25 μm to over 100 μm. Therefore, in these regions, shot peening still did have lasting beneficial effects on residual stresses after heating, even in coated specimens. The partial relaxation of compressive residual stresses from shot peening by exposures at high temperatures has been reported for similar though uncoated powder metal disk superalloys such as IN100 (Ref. 23) and Rene 95 (Ref. 15). This relaxation increased with temperature and time. Hence, the partial but not complete relaxation of compressive residual stresses in the superalloy substrate beneath the protective coating was in line with this work, although increased temperature and time would be expected to promote further relaxation of these stresses.

Test specimens were next examined after fatigue cycling that was interrupted at 14, 700, and 35,000 cycles. These cycle intervals represent 0.02, 1, and 50 percent of the average fatigue life of 70,000 cycles that had been measured at 760 °C. Cracks were only observed in the surface of the coated test specimens after the longest amount of testing at 760 °C for 35,000 cycles. Typical surface appearance after fatigue cycling is compared in Figure 6. No fatigue cracks were observed for all other combinations of fatigue test temperature and cycle intervals. The surface roughness was stable with continued fatigue cycling,

with uncoated values remaining slightly higher than those for coated test specimens, Figure 7. The associated dimpled textures and scattered laps remained as before, with no surface cracks observed to initiate specifically from these features at those intervals of fatigue cycles. However, fatigue cycling of a coated test specimen at 760 °C to 35,000 cycles produced scattered cracks which were relatively flat and normal to the axial loading direction (Fig. 6). This test condition was later reproduced on a duplicate coated test specimen, which gave the same results. These cracks ranged from 23 to 580 μm long, and had an average number density of 5.5 cracks/mm^2. Coating crack formation during fatigue cycling at certain conditions for NiCoCrAlY coatings on superalloy substrates has often been reported for turbine blade superalloys, usually attributed to the low ductility of their β NiAl phase at temperatures below about 870 °C (Ref. 12). Yet, the fatigue cracking in the present study of such a presumed ductile NiCrY coating was not previously reported or expected, and the causes of this are being further investigated.
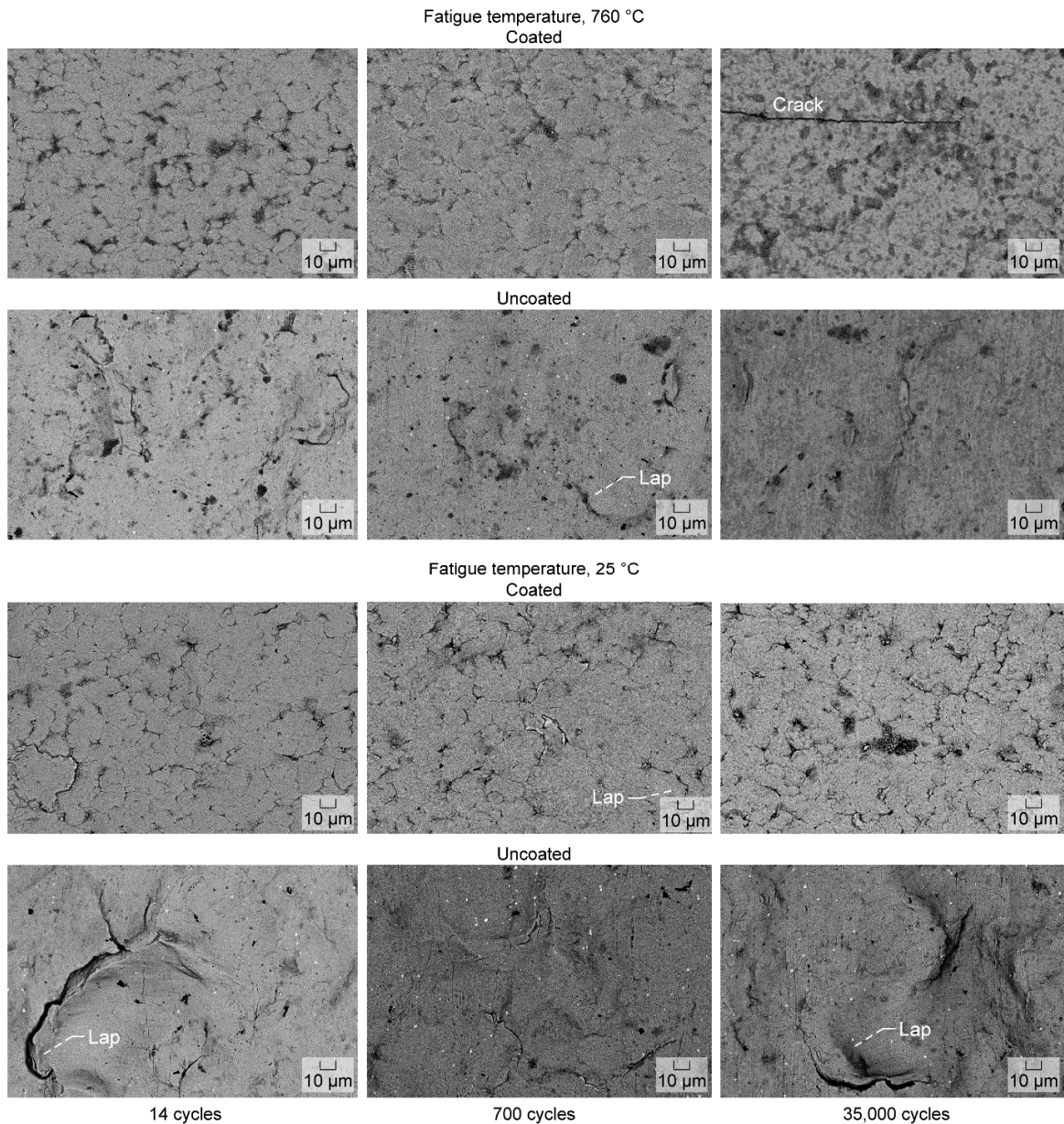

Figure 6.—Comparison of typical surface appearance after interrupted fatigue cycling. The surface appeared intact with continued fatigue in most cases, except for longest cycling at 760 °C. The fatigue loading direction is oriented vertically.
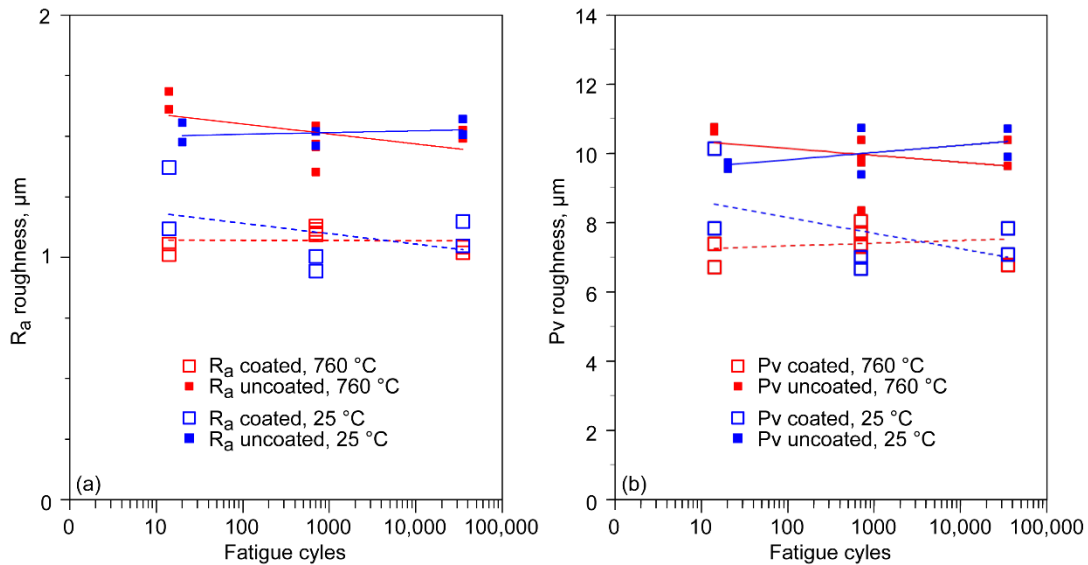
Figure 7.—Surface roughness parameters (a) R_a and (b) Pv after interrupted fatigue cycling. The surface roughness was fairly stable with continued fatigue cycling, and uncoated (hollow symbols, dashed lines) values remained slightly higher than for coated (filled symbols, solid lines).

The residual stresses measured at the surface were surprisingly stable with continued fatigue cycling in most cases, as compared in Figure 8. Residual stresses were stable for coated test specimens (hollow symbols) at both test temperatures, even when the scattered axial cracks were observed at 760 °C after cycling for 35,000 cycles. The cracks were evidently not yet frequent enough to significantly perturb these measured stresses. However, the axial residual stresses became more compressive for uncoated specimens (filled symbols) with continued cycling at 760 °C, while transverse residual stresses remained stable. So this change in axial residual stresses appeared to be driven by the fatigue cycling, as the applied loads were in this axial direction. This may be associated with cyclic hardening in this loading direction. This trend was apparent after just 700 fatigue cycles, which required only 35 min. Since the 8 h heat treatment resulted in a significant decrease in the compressive stress (Fig. 4), this increase in compressive stress indicates that the change in residual stress is due to fatigue cycling at 760 °C and not associated with the short time at this temperature. The trend was not apparent on the surface of the coated specimens.

These measurements suggested stable or even improving residual stresses remained for coated and uncoated specimens during fatigue cycling, if representative throughout the near-surface region. X-ray measurements were again repeated after electro-polishing to different depths of up to at least 100 µm from the surface, to assess stability in residual stresses near the surface. The residual stresses as a function of depth were also surprisingly stable with continued fatigue cycling in this region, as shown in Figure 9. Residual stress as a function of depth was stable for coated (filled symbols) and uncoated (hollow symbols) test specimens at both test temperatures. Increased intervals of fatigue cycles are indicated by increased symbol size, and the stress levels remained within a common band (dashed line). This was so even when the scattered axial coating cracks were observed at 760 °C after cycling for 35,000 cycles. Other studies have reported greater reductions of compressive residual stresses with initial fatigue cycles of finer grain disk superalloys IN100 (Ref. 23) and Udimet 720Li (Ref. 24), which then were stable during continue cycling. The extent of these initial reductions have been shown to depend on the specific materials mechanical properties, the plasticity resulting from prior shot peening conditions, the specific fatigue cycles, and the specific test temperature (Ref. 25). For example, fatigue cycles inducing larger plastic strains have been shown to induce greater initial reductions in these compressive residual stresses (Ref. 24). Yet, significant compressive residual stresses remained below the surface for the present conditions. Furthermore, the similarity of the present results for coated and uncoated test specimens indicates the coating did not significantly change the static and cyclic stress relaxation response in the underlying superalloy substrate, for the present test conditions.
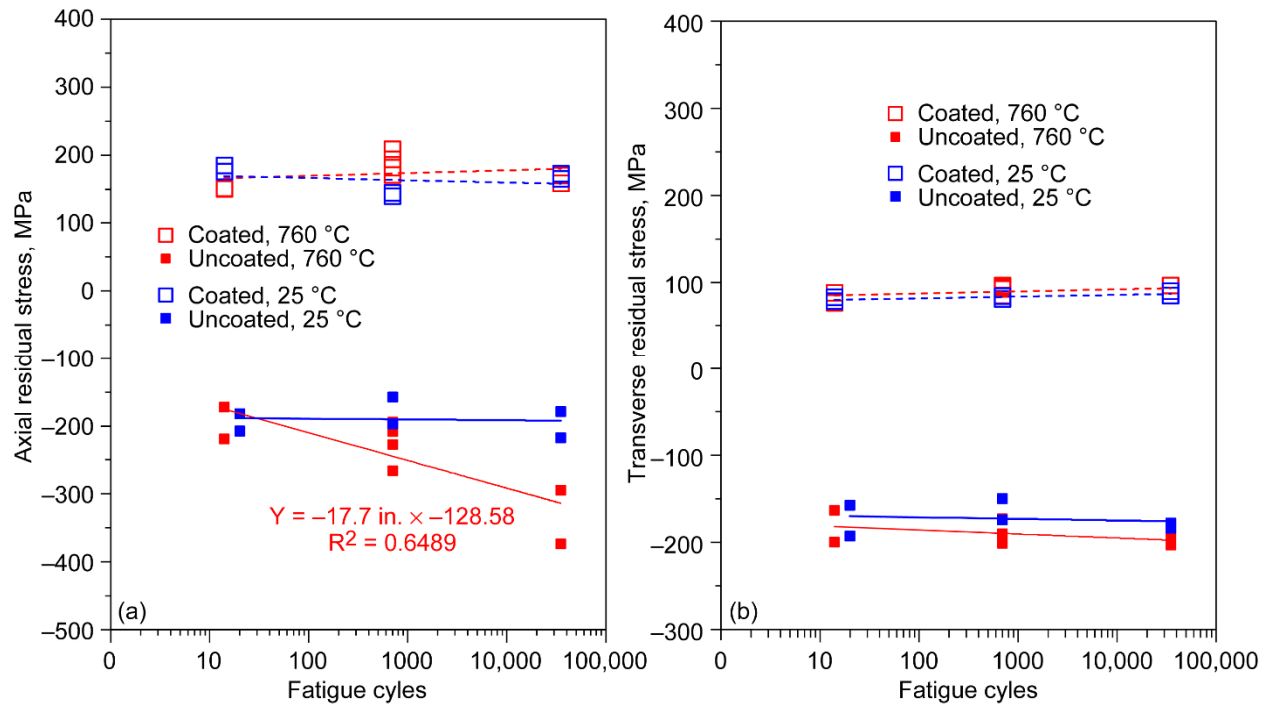
Figure 8.—Surface residual stresses in the (a) axial direction and (b) transverse direction after interrupted fatigue cycling. The surface residual stresses were stable with continued fatigue cycling in most cases including all coated specimens (hollow symbols, dashed lines), but axial stresses for uncoated specimens (filled symbols, solid lines) became more compressive at 760 °C (red symbols) with increasing cycles.
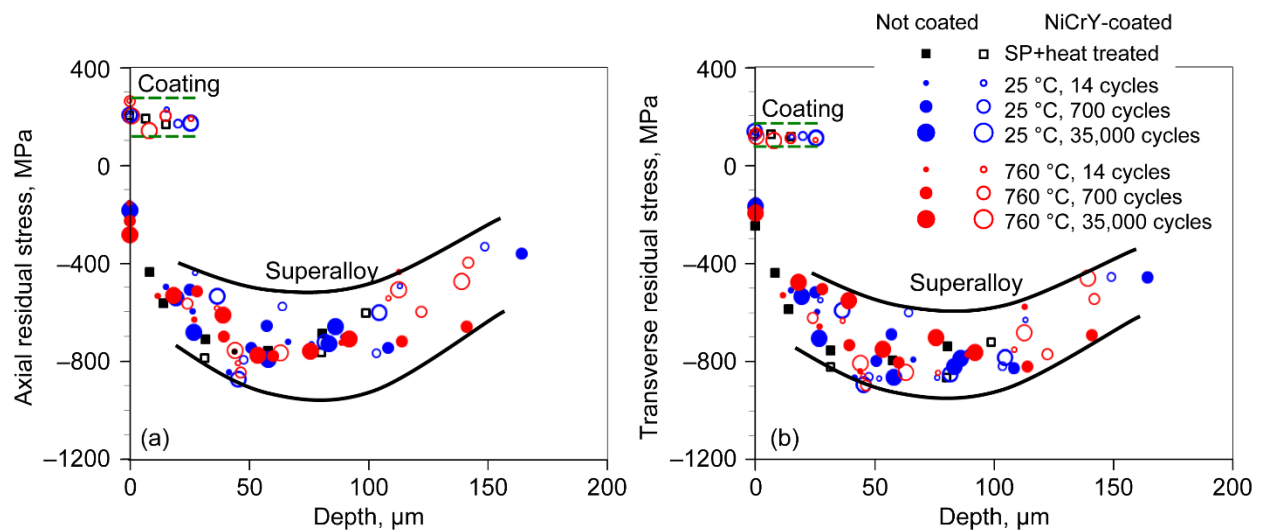

Figure 9.—(a) Axial and (b) transverse residual stresses versus depth near the surface after interrupted fatigue cycling of uncoated (filled symbols) and NiCrY-coated (hollow symbols) specimens. Residual stresses were stable (within the black band) with fatigue cycling in the coating and in the superalloy. Larger symbols indicate more fatigue cycles before interruption.
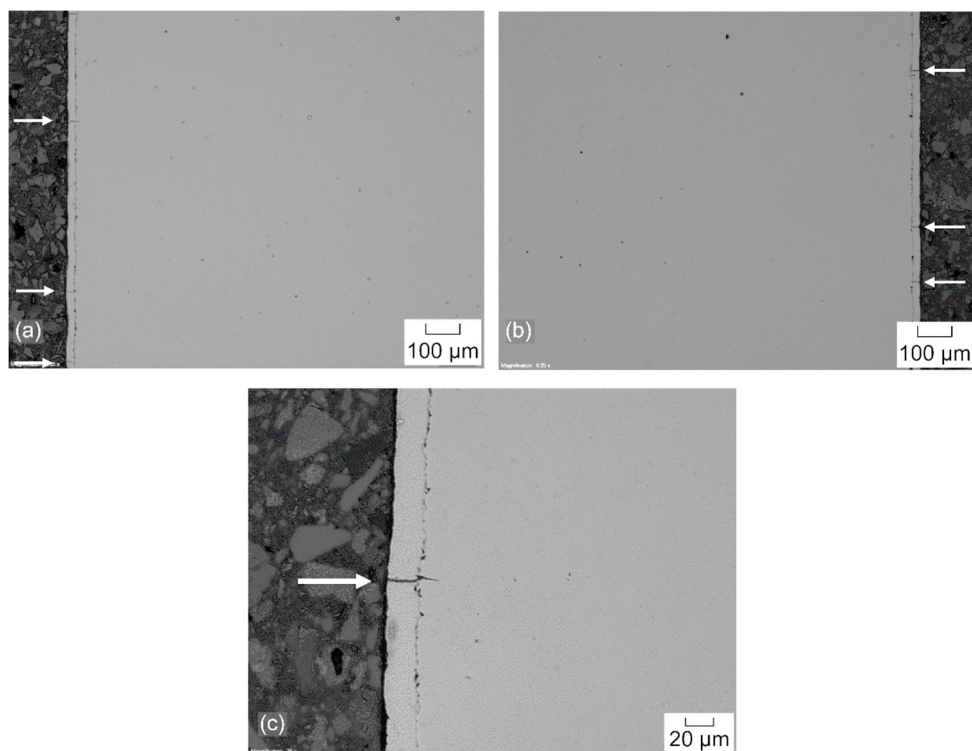
Figure 10.—Images from the longitudinal section prepared from a coated fatigue specimen after 35,000 fatigue cycles at 760 °C. The axial fatigue loads were applied in the vertical direction. Scattered cracks occurred in the coating along the specimen surface. A majority of the fatigue cracks did not penetrate into the underlying superalloy. (a), (b) typical distribution of cracks at mid-gage length; (c) deepest crack observed.

Images from a metallographic section prepared from the duplicate coated test specimen after 35,000 fatigue cycles at 760 °C are shown in Figure 10, to further examine the condition of the coating at this point. The polishing plane for this sample is parallel to the sample axis and load direction. Scattered cracks occurred in the coating along the specimen surface. However, a majority of the fatigue cracks did not penetrate into the underlying superalloy. The sectioned cracks that did continue to grow into the superalloy extended in by less than 15 μm. This apparently reflected the effects of the remaining compressive residual stresses measured in the superalloy substrate, in retarding the growth of fatigue cracks.

Images of coated and uncoated test specimen surfaces subjected to 50 h of hot corrosion with subsequent ultrasonic cleaning in water to remove any remaining salt and soluble reaction product, are shown in Figure 11. Shot peened plus heat treated test specimen surfaces are compared to those also given 35,000 fatigue cycles at room temperature or 760 °C, each then corroded 50 h. The exterior surfaces of coated and uncoated test specimens were covered in Cr_2O_3. Yet, scattered large pits exposing the substrate beneath the surface oxide were also evident in the uncoated test specimens. For the coated test specimens, the oxide was attacked in places, but no open corrosion pits exposing the substrate were observed, even for specimens fatigue tested to 700 or 35,000 cycles before hot corrosion. A higher magnification backscatter electron image (BSE) of typical sectioned samples subjected to 35,000 cycles at 760 °C and 50 h of hot corrosion are shown in Figure 12. Hence, for at least up to 50 percent of the expected LCF lifetime at 760 °C and in the presence of cracks, the coating continued to protect the superalloy substrate from corrosion attack for the conditions evaluated. It appears that after 35,000 fatigue cycles at 760 °C, the scattered fatigue cracks did not provide open sites for pits to form in the underlying superalloy. Prior work showed that even without shot peening of the coating, a similar Ni-35Cr-0.1Y (weight percent) coating still protected this superalloy from corrosion pitting after up to 1,000 h of thermal cycling between 25 and 760 °C (Ref. 16). Cold sprayed coatings of very similar composition (Ni-50Cr in weight percent) with remnant porosity have also been shown to protect steel substrates from corrosion pitting

(Ref. 26). Hence, this NiCr coating class can continue to protect substrates from corrosion in spite of some levels of flaws, including the porosity, oxidation, or fatigue cracking observed for these cases.

In further support of this, a polished cross-section with the present coating on a separate fatigue test specimen with the same shot peening and heat treatment is shown for comparison in Figure 13. This specimen was then subjected to oxidation exposure in air for 500 h at 760 °C and the hot corrosion test as above, followed by fatigue cycling to failure at 760 °C, using the same applied stresses as before. The polishing plane for this test specimen was again parallel to the loading direction. Cracks can be seen penetrating the coating but again show minimal extension into the substrate. Only the outer portion of the sample still contains the high-Cr alpha phase. Interdiffusion with the substrate, likely during the 500 h oxidation exposure, has resulted in recession of the alpha phase. Multiple secondary fatigue cracks grew through the coating, but many still did not extend into the underlying superalloy. Again, no corrosion pits were found that penetrated the coating during the corrosion treatment. Therefore, the coating did appear to be robust, in still protecting the substrate superalloy from corrosion attack and pit formation for the present conditions in the presence of these changes from extended oxidation exposures.
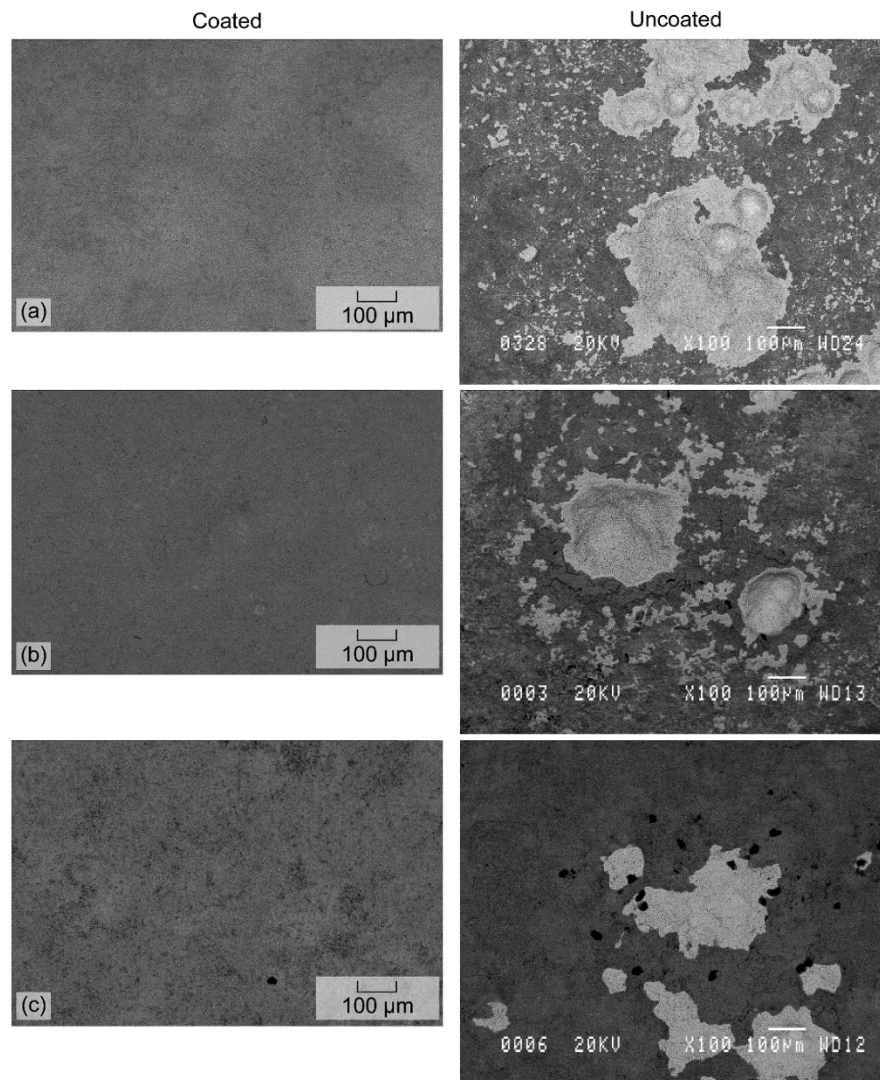

Figure 11.—Comparisons of typical surface appearance of coated and uncoated test specimens after hot corrosion at 760 °C for 50 h, after: (a) no fatigue cycles, (b) 35,000 fatigue cycles at room temperature, (c) 35,000 fatigue cycles at 760 °C. The coating prevented corrosion from exposing the substrate after even 35,000 fatigue cycles, with no open pits observed. The axial fatigue loads had been applied in the horizontal direction.
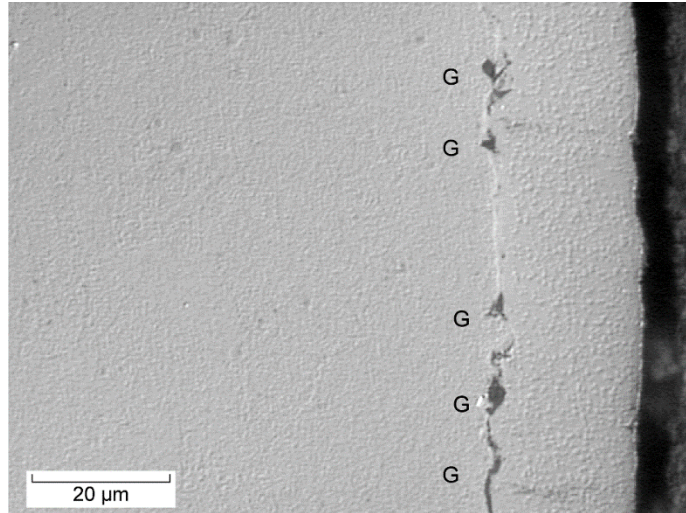
Figure 12.—Longitudinal section prepared from a coated fatigue specimen after 35,000 fatigue cycles at 760 °C, plus 50 h of hot corrosion at 760 °C. G-alumina grit particles embedded during grit blasting, before the coating process. The coating did not show pits extending into the underlying superalloy. The axial fatigue loads had been applied in the vertical direction.
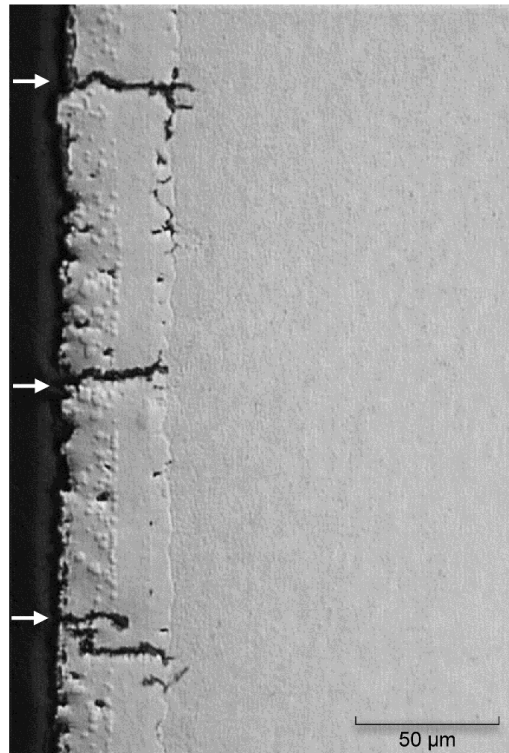

Figure 13.—Secondary cracks observed in longitudinal section prepared from a coated fatigue specimen that was subjected to 500 h of oxidation at 760 °C plus 50 h of hot corrosion at 760 °C, and then fatigue tested at 760 °C to failure. Multiple secondary fatigue cracks grew through the coating, but many still did not extend into the underlying superalloy. The axial fatigue loads were applied in the vertical direction.

Summary of Results

LSHR fatigue test specimens were coated with a NiCrY coating, and then shot peened and heat treated along with uncoated test specimens. Shot peening made average roughness more uniform, but the induced compressive residual stresses relaxed at the surface during subsequent heat treatment for both coated and uncoated test specimens. Residual stresses at the surface of coated specimens became slightly tensile after this heat treatment. Yet, significant compressive residual stresses remained below the surface in the substrate for both the coated and uncoated cases. Following shot peening and heat treatment, both coated and uncoated specimens were fatigue cycled at room temperature and at 760 °C for up to half the average LCF lifetime previously measured at 760 °C. For both the coated and uncoated case, the surface roughness and residual stresses remained stable, except that the axial residual stress at the surface for the uncoated specimen became more compressive with continued cycling at 760 °C. In addition, for the coated sample, cracks appeared in the coating after the longest period of cycling (35,000 cycles) at 760 °C. Following the fatigue cycling, sections of each sample were corroded at 760 °C for 50 h. Corrosion pits were observed to form on the uncoated samples. However, although the thin surface oxide was attacked on the coated samples, no corrosion pits were observed even where fatigue cracks existed in the coating.

Conclusions

1. Shot peening can make the roughness of coatings more uniform, but the induced compressive residual stresses at the surface can relax at high temperatures. Yet, substantial compressive residual stresses can still remain below the surface in the substrate.
2. The shot peened surface can remain intact during continued fatigue cycling with stable roughness and residual stresses for most cases, except for longest cycling at 760 °C:
    a. For uncoated test specimens, axial residual stresses can become more compressive with cycling, and surface cracking is not expected until after 35,000 cycles.
    b. For coated specimens, cracks can begin to form sooner in the coating, consistent with the lack of these compressive residual stresses in the coating. Yet, the adjacent substrate can retain stable compressive residual stresses, sufficient to continue suppressing fatigue crack growth into the substrate.
3. Corrosion resistance in air at 760 °C for 50 h was not strongly impacted by this fatigue cycling:
    a. For uncoated specimens, the oxide layers formed during such intervals of fatigue cycling at 760 °C are not sufficiently protective to prevent corrosion pits from still reaching the substrate.
    b. For coated specimens, the NiCrY coating can remain protective after these intervals of fatigue cycling to continue preventing these pits from forming, even when fatigue cracks have begun to form, or after extended oxidation.

References

1. R. Schafrik, R. Sprague, "Superalloy Technology–A Perspective on Critical Innovations for Turbine Engines," Key Engineering Materials, V 380, 2008, pp. 113–134.
2. M.R. Bache, J.P. Jones, G.L. Drew, M.C. Hardy, N. Fox, "Environment and Time Dependent Effects on the Fatigue Response of an Advanced Nickel Based Superalloy," Int. J. Fat., V 31 (11–12), 2009, pp. 1719–1723.
3. A. Encinas-Oropesa, G. Drew, M. Hardy, A. Leggett, J. Nicholls, and N. Simms, "Effects of Oxidation and Hot Corrosion in a Nickel Disc Alloy," Superalloys 2008, ed. R.C. Reed, K.A. Green, P. Caron, T.P. Gabb, M.A. Fahrmann, E.S. Huron, S.A. Woodard, The Mining, Metallurgy, and Materials Society, Warrendale, PA, 2008, pp. 609–618.

4. C.K. Sudbrack, S.L. Draper, T. Gorman, J. Telesman, T.P. Gabb, D.R. Hull, "Oxidation and the Effects of High Temperature Exposures on Notched Fatigue Life of an Advanced Powder Metallurgy Disk Superalloy," Superalloys 2012, E.S. Huron, R.C. Reed, M.C. Hardy, M.J. Mills, R.E. Montero, P.D. Portella and J. Telesman, Eds., TMS, Warrendale, PA, 2012, pp. 863–872.
5. R.A. Rapp, "Hot Corrosion of Materials: A Fluxing Mechanism?" Corros. Sci., 2002, 44, pp. 209–221.
6. F.S. Pettit and C.S. Giggins, "Hot Corrosion," Superalloys II, C.T. Sims, N.S. Stoloff, and W.C. Hagel, Eds., John Wiley & Sons, New York, 1987, pp. 327–358.
7. B. Gleason, "High-Temperature Corrosion of Metallic Alloys and Coatings," Materials Science and Technology, ed. R.W. Cahn, P. Haasen, E.J. Kramer, John Wiley & Sons Inc., 2000, pp. 173–228.
8. J.R. Groh and R.W. Duvelius, "Influence of Corrosion Pitting on Alloy 718 Fatigue Capability," Superalloy 718, 625, 706 and Derivatives, ed. E.A. Loria, The Mining, Metallurgy, and Materials Society, Warrendale, PA, 2001, pp. 583–592.
9. G.S. Mahobia, N. Paulose, S.L. Mannan, R.G. Sudhakar, K. Chattopadhyay, N.C.S. Srinivas, "Effects of Hot Corrosion on the Low Cycle Fatigue Behavior of IN718," Int. J. Fat., V. 59, 2014, pp. 272–281.
10. J.K. Sahu, R.K. Gupta, J. Swaminathan, N. Paulose, S.L. Mannan, "Influence of Hot Corrosion on the Low Cycle Fatigue Behavior of SU 263," Int. J. Fat., V. 51, 2013, pp. 68–73.
11. J. Telesman, T.P. Gabb, Y. Yamada, S.L. Draper, "Fatigue Resistance of a Hot Corrosion Exposed Disk Superalloy at Varied Test Temperatures," Mat. at High Temperatures, V. 33 (4-5), 2016, pp. 517–527.
12. G.W. Goward, "Progress in Coatings for Gas Turbine Airfoils," Surface and Coatings Technology, V 108–109, 1998, pp. 73–79.
13. G. Kappmeyer, C. Hubig, M. Hardy, M. Witty, M. Busch, "Modern Machining of Advanced Aerospace Alloys – Enabler for Quality and Performance," 5th CIRP Conference on High Performance Cutting 2012, Elsevier B.V., Amsterdam, The Netherlands, 2012, pp. 28–43.
14. P.S. Prevéy "X-Ray Diffraction Characterization of Residual Stresses Produced by Shot Peening," Shot Peening Theory and Application, ed. A. Niku-Lari, IITT-International, Gournay-Sur-Marne, France, 1990, pp. 81–93.
15. M.K. Tufft, "Shot Peen Impact on Life, Part 1: Development of a Fracture Mechanics/Threshold Behavior Predictive Model," Shot Peening Present & Future, Proc. Of the 7th International Conference on Shot Peening, Institute of Precision Mechanics, 1999, pp. 244–253.
16. T.P. Gabb, R.A. Miller, C.K. Sudbrack, S.L. Draper, J.A. Nesbitt, R.B. Rogers, J. Telesman, V. Ngo, J. Healy, "Cyclic Oxidation and Hot Corrosion of NiCrY-Coated Disk Superalloys," NASA/TM—2016-219105, Washington, D.C., June, 2016.
17. J.T. Cammet, P.S. Prevéy, N. Jayaraman, "The Effect of Shot Peening Coverage on Residual Stress, Cold Work, and Fatigue in a Nickel-Base Superalloy," Proceedings of ICSP-9, ed. V. Schulze, A. Niku-Lavi, 2005.
18. M.G. Moore, W.P. Evans, "Mathematical Correction for Stress in Removed Layers in X-Ray Diffraction Residual Stress Analysis," SAE Transactions, V. 66, 1958, pp. 340–344.
19. J. Nesbitt, S.L. Draper, "Pit Morphology and Depth After Low-temperature Hot Corrosion of a Disc Alloy," Mat. at High Temperatures, V. 51 (4–5), 2016, pp. 501–516.
20. N. Bala, H. Singh, S. Prakash, "X-ray Diffraction Study of Cold Sprayed Ni-20Cr and Ni-50Cr Coatings on Boiler," Advanced Materials Research, V. 620, 2013, pp. 257–262.
21. J.F. Loersch, J.W. Neal, "Peened Overlay Coatings," U.S. 4,514,469, U.S. Patent Office, Washington, D.C., 1985.
22. B.T. Hazel, M.J. Weimer, "Turbine Component Protected With Environmental Coating," U.S. 7,364,801 B1, U.S. Patent Office, Washington, DC, 2008.
23. D. Buchanon, R. John, R.A. Brockman, A.H. Rosenberger, "A Coupled Creep Plasticity Model for Residual Stress Relaxation of a Shot Peened Nickel-Base Superalloy," Superalloys 2008, ed. R.C. Reed, K.A. Green, P. Caron, T.P. Gabb, M.A. Fahrmann, E.S. Huron, S.A. Woodard, The Mining, Metallurgy, and Materials Society, Warrendale, PA, 2008, pp. 965–974.

24. A. Evans, S-B. Kim, J. Shackleton, G. Bruno, M. Preuss, P.J. Withers, "Relaxation of Residual Stress in Shot Peened Udimet 720Li Under High Temperature Isothermal Fatigue," Int. J. Fat., V. 27, 2005, pp. 1530–1534.
25. W.Z. Zhuang, G.R. Halford, "Investigation of Residual Stress Relaxation Under Cyclic Load," Int. J. Fat., V. 23(1), 2001, pp. 31–37.
26. N. Bala, H. Singh, J. Karthikeyan, S. Prakash, "Cold Spray Coating Process for Corrosion Protection: a Review," Surface Engineering, V. 30(6), 2014, pp. 414–421.